5. COMPARISON BETWEEN ALLOWABLE STRAINS AND EXPERIMENTAL FRACTURE STRAINS

5.1 Calculation of Allowable Strains

The purpose of this section is to assess the degree to which the various defect tolerance criteria can be used to establish safe operating conditions for pipeline girth welds. To accomplish this, the methodologies on which the various criteria are based (Table 5.1) were applied to selected, full-scale pipe fracture tests described in the preceding section to calculate allowable applied strain. This was done because it is not possible to apply the defect assessment standards described in Section 3 to the pipe fracture data because of the many additional constraints they impose. For example, API 1104 Appendix A requires a minimum CTOD toughness of 0.127 mm (0.005 in.) measured at 15°C below the operating temperature, in this case the test temperature. There are no data which satisfy this criterion.

Table 5.1 Methodologies used in the Comparison of Allowable Strains and Experimental Fracture Strains .

Methodology:	1.	COD Design Curve With Only Residual Strain Correction.
	2.	COD Design Curve With Only Defect Geometry Correction.
	3.	COD Design Curve With Residual Strain and Defect Geometry Correction.
	4.	COD Design Curve With CSA Z184 Appendix K Defect Geometry Correction and Collapse Criterion.
	5.	NBS Approach

Methodology 1: This methodology is the COD Design Curve, equation 3.1, with the value of e equal to the sum of the externally applied strain plus a residual strain taken equal to the weld yield strength divided by Young's Modulus: E-207GPa (30 x 10^6 psi). The defect depth is used directly for $\bar{a}$; there is no modification for defect geometry. This methodology is similar to API 1104 Appendix A. The important differences are that Appendix A limits the defect length to $\ell < 0.4D$ ($0.127\pi D$) for $a/t < 0.25$ and $\ell < 4t$ for $0.25 < a/t \leq 0.5$; defects with $a/t > 0.5$ are not allowed. In addition, Appendix A calculates allowable defect depths or applied strains using only two toughness levels, depending on the toughness of the weld, and requires that CTOD toughness exceed 0.127 mm (0.005 in.) at 15°C below the operating temperature. Finally, API 1104 Appendix A imposes a residual strain of 0.2 percent independent of the material properties.

Methodoloev 2: This methodology is the COD Design Curve, equation 3.1, with the value of e taken as the externally applied strain and with $\bar{a}$ determined from the geometry correction curves. No residual strain is included. These curves can be found in PD 6493 and correspond to the linear elastic Newman-Raju K_A solutions; see also Figure B1 of Appendix B. This methodology is included to assess the effect of only using a geometry correction in conjunction with the COD Design Curve.

Methodology 3: This methodology is the COD Design Curve with both the residual strain correction of Methodology 1 and the geometry correction of Methodology 2. It is similar to the methodology employed by BS 4515 Appendix H. The important differences are that: Appendix H does not permit initial defects that are believed to be cracks, which implicitly eliminates defects deeper that one weld pass, 3 mm (0.12 in.); the defect length is limited by a plastic collapse criterion; and the minimum CTOD toughness is about 0.08 mm (0.003 in.).

Methodology 4: This is the COD Design Curve, equation 3.1, with the defect geometry correction and collapse criterion used in CSA 2184 Appendix K. No residual strain is included. This methodology is almost

identical to CSA 2184 Appendix K. The differences are that Appendix K allows no cracks and defect length is limited to $0.1(\pi D)$.

Methodoloev 5; **NBS** methodology. The computer program written by **NBS** was loaded onto our PDP11/23 and used to calculate allowable strains. However, some difficulty was encountered in applying the program for this purpose since it is designed to compute allowable defect depth versus length curves for a particular pipe configuration, toughness and applied stress. Consequently, only a limited set of calculations were made. In all of these, it was assumed that $\sigma_o = \sigma_f = 483$ MPa (70 ksi) and that the reduction in effective CTOD toughness due to residual stress was 0.025 mm (0.001 in.). Stress was converted to strain by dividing by E = 207 GPa (30×10^6 psi).

The data used in the calculations are listed in Table 5.2 and shown graphically as a/t versus $\ell/\pi D$ in Figure 5.1. Also shown in Figure 5.1, for comparison, are limits on initial defect size required by API 1104 Appendix A, **BS** 4515 Appendix H, and CSA 2184 Appendix K for specific pipe geometries. Very few points fall within the limits of API 1104 Appendix A and **BS** 4515 Appendix **H.** The data points that meet the geometric limitations of the proposed criteria are:

API 1104 Appendix A	16, 17, A6, A8, I1, 12, 3
BS 4515 Appendix H	A8, I1, 12, 3
CSA 2184 Appendix K	7, 14, 15, 18, 19, Al, A3, A5, A6, A7, A8, I1, 12, 1, 3

The results of the calculations are also shown in Table 5.2 which lists most of the information required for the calculations. Further details can be found in Section 4. The calculated allowable strains are listed by methodology number (Table 5.1); a key is given in the table for convenience. Some of the calculations involving the inclusion of a residual strain, result in a negative calculated allowable strain. These cases correspond to a total allowable strain which is less than

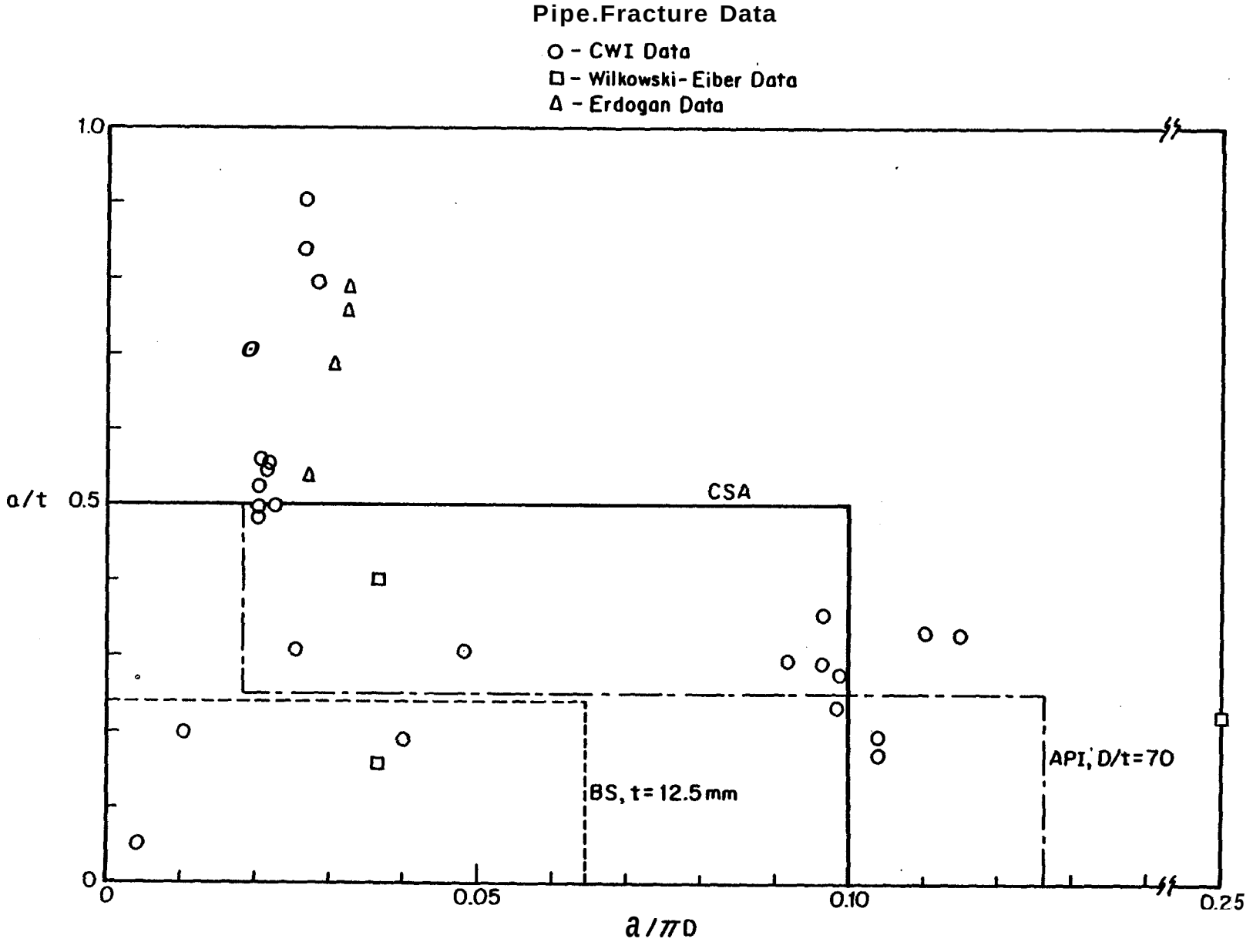

Figure 5.1 Summary of Data Used to Compare Methodologies with Bounds Placed on Initial Defect *Sizes* from the Three Standards

Table 5.2 Allowable Applied Strains for Actual Pipeline Girth Weld Defects

Test[Ref.]	D(mm)	t(mm)	a(mm)	ℓ(mm)	δ(mm)	σ_o(MPa)	e_f(%)	e_a(%) 1	2	3	4	5
6[20]	914	11.1	7.8	68.6	0.024	524	0.33	-0.14	0.08	-0.17	0.08	
7[20]	914	11.1	5.3	61.0	0.024	524	0.31	-0.12	0.10	-0.15	0.09	
8[20]	914	11.1	10.1	76.4	0.024	524	0.14.	-0.15	0.08	-0.18	0.07	
9[20]	914	11.1	8.8	81.8	0.089	524	0.48	-0.03	0.11	-0.14	0.12	
10[20]	914	11.1	6.4	59.3	0.024	524	0.23	-0.13	0.09	-0.16	0.09	
11[20]	914	11.1	9.3	78.9	0.089	524	0.49	-0.04	0.12	-0.13	0.11	
12[20]	914	11.1	6.3	63.5	0.089	524	>0.5	0.03	0.16	-0.09	0.16	
13[20]	914	11.1	6.1	62.2	0.089	524	0.36	0.04	0.17	-0.08	0.18	
14[20]	914	11.1	5.5	64.8	0.10	524	0.51	0.09	0.19	0.06	0.14	0.16
15[20]	914	11.1	5.5	60.3	0.10	524	0.47	0.09	0.19	0.06	0.16	0.17
*16[20]	914	10.3	2.0	300	0.10	690	>0.78	0.53	0.70	-0.37	0.10	0.15
*17[20]	914	10.3	1.8	300	0.10	690	>0.71	0.64	0.86	0.53	0.11	0.16
18[21]	914	11.1	3.3	265	0.10	524	0.30	0.29	0.24	-0.02	0.10	0.17
19[21]	914	11.1	3.2	278	0.10	524	0.37	0.29	0.24	-0.02	0.10	0.17
A1[21]	914	11.1	3.93	279	0.10	469	0.20	0.24	0.18	-0.05	0.07	0.15
A2[21]	914	11.1	3.70	331	0.10	469	0.20	0.24	0.18	-0.05	0.07	0.16
A3[21]	914	11.1	3.50	75	0.10	469	0.49	0.27	0.29	0.06	0.20	0.18
A4[22]	914	11.1	3.7	315	0.10	441	0.27	0.26	0.19	-0.02	0.09	0.16
A5[22]	914	11.1	3.1	282	0.10	469	0.32	0.35	0.29	0.06	0.11	0.17
A6[22]	914	11.7	2.9	280	0.10	469	0.35	0.35	0.33	0.10	0.14	0.18
A7[22]	914	11.7	3.7	134	0.10	469	0.31	0.24	0.21	-0.02	0.13	0.17
A8[22]	914	11.7	2.2	116	0.10	469	0.65	0.52	0.44	0.22	0.20	0.20
I1[21]	1067	15	0.9	14	0.10	497	>0.7	1.37	1.30	1.06	0.25	0.23
I2[21]	1067	15	3.0	38	0.10	497	>0.8	0.34	0.45	0.21	0.23	0.23
I3[21]	1067	15	8.0	70	0.10	497	0.62	0.02	0.26	0.02	0.16	0.14
1[24]	762	15.9	6.4	89	0.05	524	0.24	-0.02	0.11	-0.09	0.11	0.09
2[24]	762	15.9	3.2	599	0.05	524	0.17	0.10	0.19	-0.01	0.13	0.14
3[24]	762	15.9	2.5	89	0.05	524	>0.64	0.17	0.26	0.06	0.23	0.17

Methodology
1. COD-Design Curve with residual strain
2. COD-Design Curve with geometry correction
3. COD-Design Curve with residual strain and geometry correction
4. COD-Design Curve with CSA geometry correction and collapse criterion
5. * NBS
Buried defects

the assumed residual strain and are not plotted in the figures that follow.

Figures 5.2 through 5.7 present the results in graphical form for the individual methodologies. The data are plotted as failure strain versus allowable strain, both normalized by the weld yield strain or base metal yield strain in the cases for which base metal was tested. Lines corresponding to safety factors (SF) equal to one and two are drawn on the figures for comparison. These are safety margins on strain with respect to failure. In many cases crack growth initiated at applied strains significantly lower than the failure strains (see Table 4.4). There are also plots for two of the methodologies of the ratio e_f/e_a versus a/R to highlight the effect of defect aspect ratio. Data points with an arrow correspond to tests terminated before failure or to data off the scale of the plot.

Figure 5.2 shows the results of Methodology 1, which is the COD Design Curve with only a residual strain correction and is similar to API 1104 Appendix A. Concentric circles correspond to multiple data points. The figure shows that the methodology is conservative for all but three points. The safety factor is approximately one, but there is a great deal of scatter. Figure 5.3, which is a plot of the ratio of failure strain to allowable strain verses defect aspect ratio, a/ℓ, shows that the nonconservative allowable strains, and generally the safety factors near unity, correspond to defects which are long in comparison to their depth.

Figure 5.4 shows the results of Methodology 2, which is the COD Design Curve with only the defect geometry correction of PD 6493. The results show that, with one exception, the allowable strains are conservative. In addition, there is less scatter in the safety factors when only the geometry correction is used instead of only the residual strain. Figure 5.5 shows the data plotted as e_f/e_a versus a/ℓ. From this curve, one notes a definite influence of defect aspect ratio on the safety factor even with the inclusion of the defect geometry

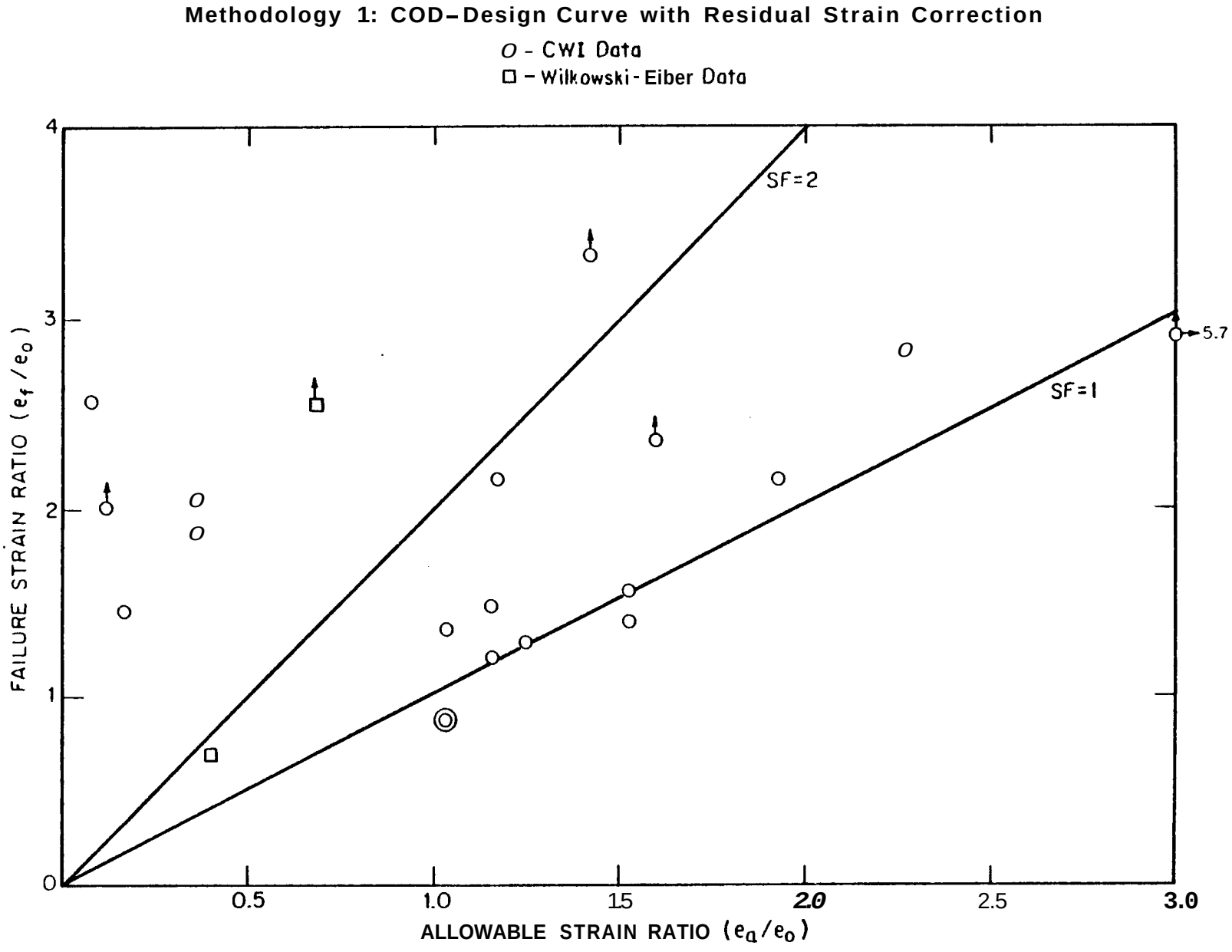

Figure 5.2 Fracture Strain vs Allowable Strain Calculated According to Methodology 1

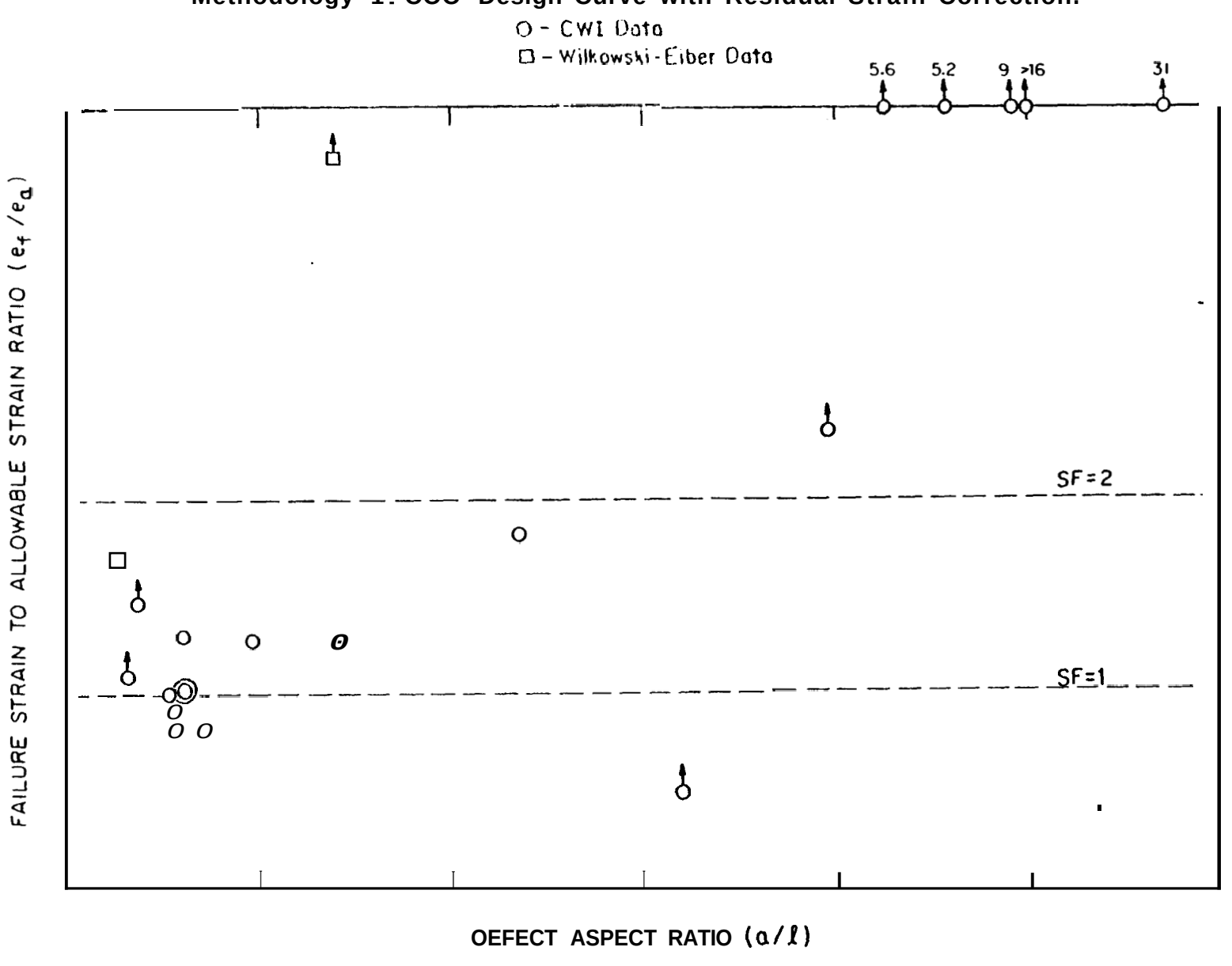

Figure 5.3 Fracture Strain to Allowable Strain Ratio vs Defect Aspect Ratio for Methodology 1

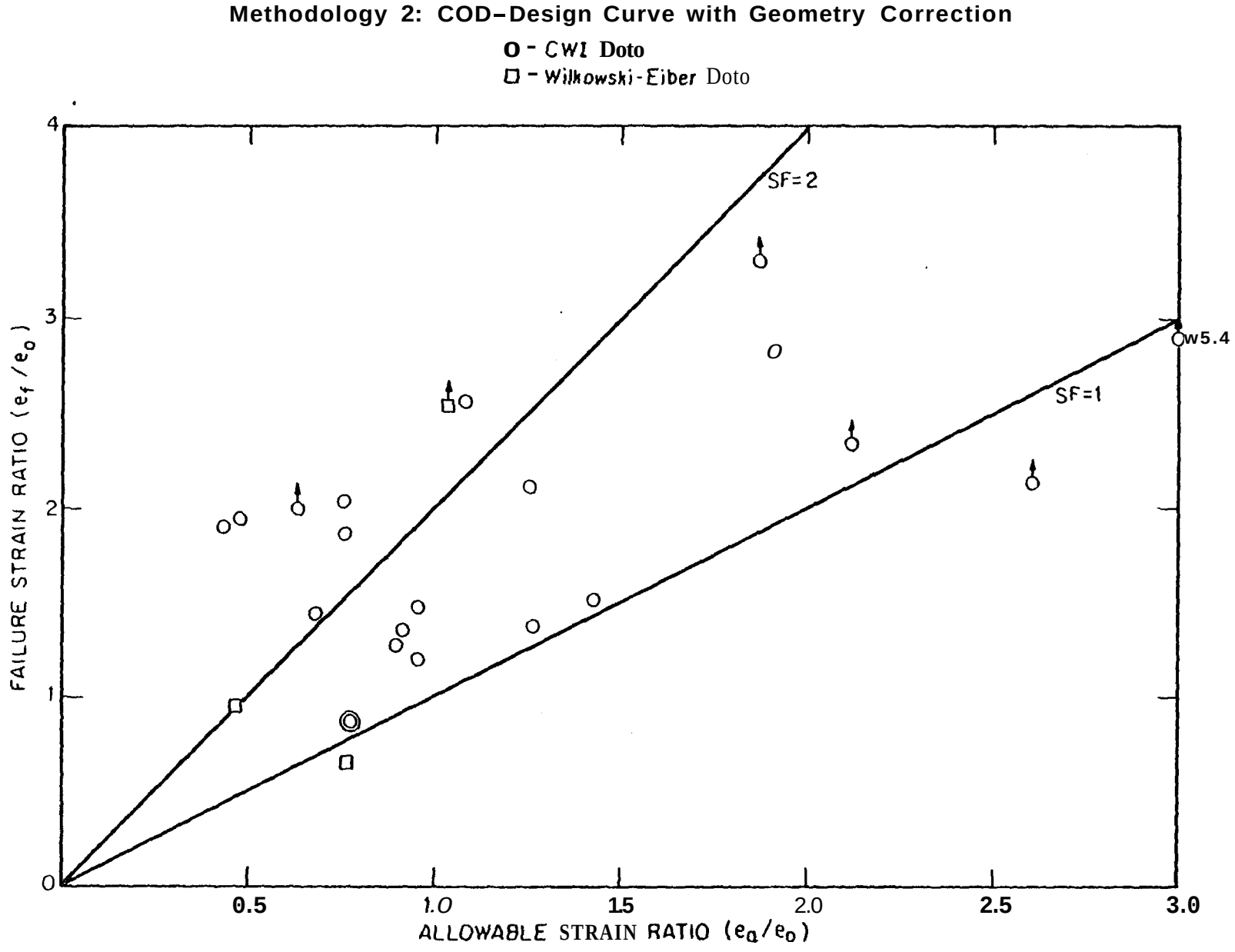

Figure 5.4 Fracture Strain vs Allowable Strain Calculated According to Methodology 2

Methodology 2: COD–Design Curve with Geometry Correction.

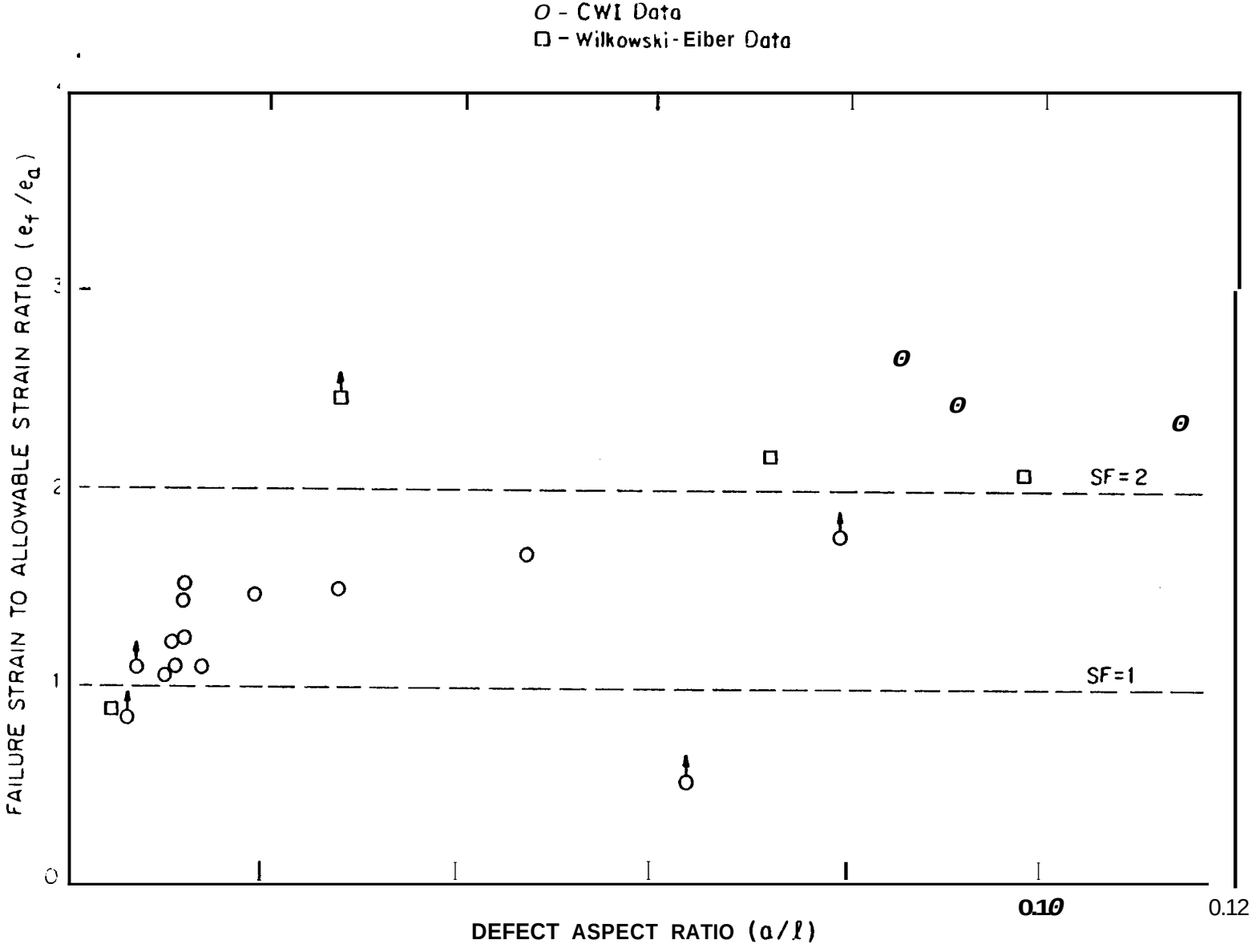

Figure 5.5 Fracture Strain to Allowable Strain Ratio vs Defect Aspect Ratio for Methodology 2

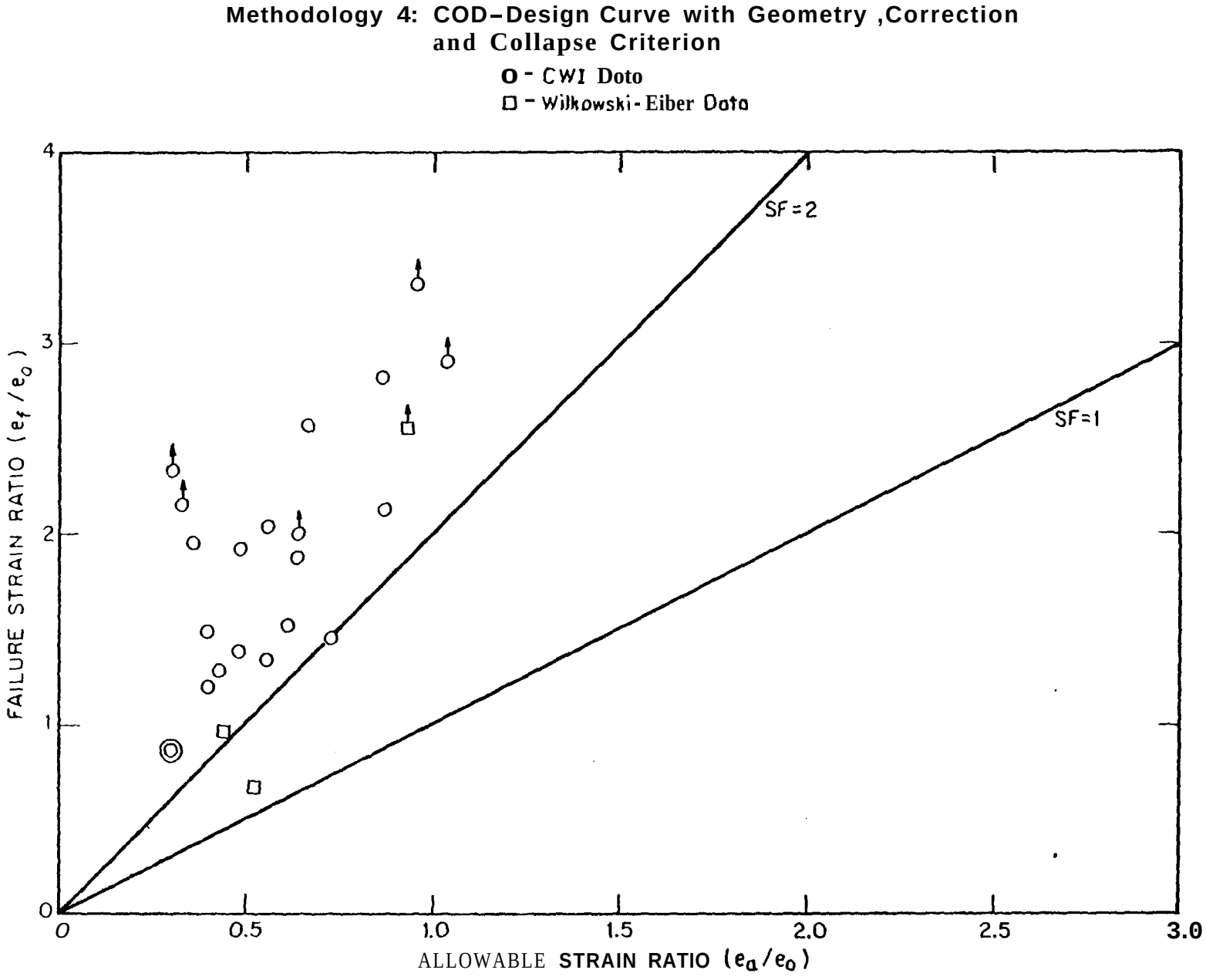

Figure 5.6 Fracture Strain vs Allowable Strain Calculated According to Methodology 4

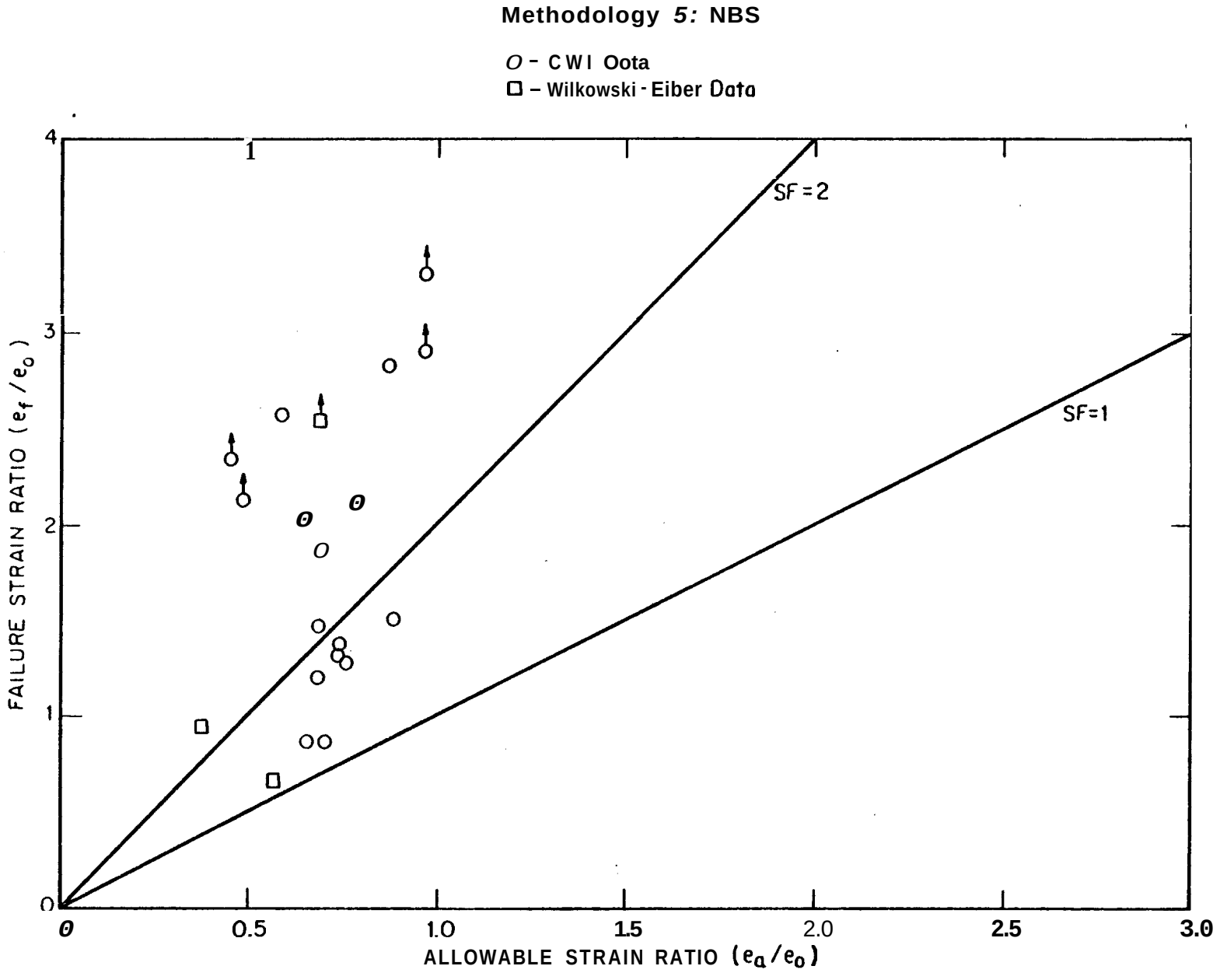

Figure 5.7 Fracture Strain vs Allowable Strain Ratio vs. Defect Aspect Ratio for Methodology 5

correction. This observation has been reported before [27] and is discussed later in this section and in Appendix B.

No figure is given for Methodology 3 which is the COD Design Curve with both residual strain and defect geometry corrections. The reason can be seen in Table 5.2 which shows that for virtually every case, no externally applied strain is allowed. Methodology 3 is similar to BS 4515 Appendix H and indicates that this standard is very conservative.

Figure 5.6 shows the results of Methodology 4, which is almost identical to CSA 2184 Appendix K. The results show that the methodology is conservative by a factor of two, with only one exception which is nevertheless conservative. This figure is no surprise since the CSA standard includes empirical defect geometry correction curves which were based on most of the same data and is designed to give a safety factor of two.

Figure 5.7 shows the NBS methodology results, which are seen to be conservative in all cases. The allowable strain is almost always between 0.5 and 1.0 times the yield strain. The NBS methodology is meant to predict failure strains, as opposed to providing allowable strains. The results show that the predicted failure strains are conservative and sometimes underestimate the measured values by more than a factor of two.

5.2 Discussion of Results and Their Implications for the Proposed Defect Tolerance Criteria

Results have been presented for various defect tolerance assessment approaches which are based on the COD Design Curve. They are each distinct in their treatment of crack geometry correction, residual stress influence, and on imposition of additional constraints based on plastic collapse considerations. The comparison of allowable strain levels for each method with observed failure strains shows that by accounting for crack geometry, plastic collapse, and residual stress one can ensure that the allowable strains are consistently less than the

measured failure strains. The methods for treating each of these effects are approximate, and improvements in these methods would lead to more accurate defect tolerance criteria.

In particular, the geometry correction used in PD 6493 and incorporated into BS 4515 Appendix H is based on elastic analysis while its application to pipeline girth welds usually involves elastic-plastic conditions. The inaccuracy of this crack geometry correction is evidenced by the aspect: ratio effect seen in Figure 5.5, which contains COD Design Curve predictions already including the elastic crack geometry correction. In CSA 2184 Appendix K, the curves used to adjust for crack geometry have been empirically altered from those calculated using elastic geometry corrections. The influence of plasticity on crack geometry corrections io discussed more fully in Appendix B, where quantitative estimates are presented for example conditions.

Residual stresses are believed to influence the level of applied strain which causes failure, and adjustment of the COD Design Curve for residual stress generally increases the safety margin. The adjustment is made by adding a residual stress or strain equal to the corresponding yield value to the applied stress or strain and entering the total stress or strain into the COD Design Curve. The results given in Table 5.2 for Methodology 3 indicate that such a residual stress correction coupled with a geometry correction approach often reduces the allowable applied stresses or strains drastically. The use of such a residual stress correction increases the safety margin but does not reduce the data scatter. Residual stress corrections are included in the API 1104 Appendix A and the BS 4515 Appendix H. The CSA 2184 Appendix K does not include a residual stress correction factor. Actual residual stresses are generally less than yield and their influence on failure stress is dependent on the amount of plastic deformation which precedes or accompanies failure.

The COD Design Curve does not account for the possibility of plastic collapse and allows for strain levels which correspond to full yielding of the section. Its use without additional plastic collapse

constraints may result in nonconservative estimates of allowable strain in this regime. Both BS 4515 Appendix H and CSA 2184 Appendix K include plastic collapse-based limitations on allowable strain and defect size. Each uses a different plastic collapse calculation procedure and both methods are approximate, conservative, and somewhat empirical.

The results obtained in this study indicate that if the COD Design Curve is used with the elastic crack geometry correction, residual stress correction and plastic collapse limitation, conservative estimates of allowable strain are ensured. The BS 4515 Appendix H is developed on that basis. On the other hand, CSA 2184 Appendix K produces allowable strain estimates which are consistently conservative without including a residual stress correction but using data to empirically adjust the elastic geometry correction.

API 1104 Appendix A is based on Methodology 1 but with additional restrictions on defect size and toughness. None of the data reviewed meets the toughness requirement. Only a portion of the data in Table 5.2 is within the allowable defect size limit. Considering all the data evaluated, Methodology 1 has a strong aspect ratio influence on safety margin and little or no safety margin for long flaws. If only the data within the API 1104 Appendix A defect size restriction is considered, seven points remain, only one of which corresponds to a ductile‘tearing mode of failure. The other data points correspond to buckling or to stopping of the test without reaching final failure. For the point (A6), which satisfies the API 1104 Appendix A geometry limitations and failed by ductile tearing the safety margin on failure strain is 1.0 and crack growth initiated at less than 50 percent of the allowable strain as determined by Methodology 1. This data point has a crack depth to pipe thickness ratio of 0.25 and a crack length to pipe circumference ratio 0.10.

The NBS methodology for setting allowable girth weld defect sizes, which is not based on the COD Design Curve, is found to be conservative for each of the cases considered here. This methodology employs the

crack tip opening displacement as the fracture parameter and incorporates a residual strain correction but no specified safety margin. The procedure for calculating CTOD involves an elastic-perfectly plastic model of material behavior.

Two trends are observable in comparing the NBS predictions for failure strains to the measured data. First, there is an apparent aspect ratio effect on the safety margin with low aspect ratio (a/ℓ) defects having smaller safety margins than higher aspect ratio defects. This effect may be due to a constraint influence on the apparent toughness of the material, by which crack growth occurs for low aspect ratio (a/ℓ) defects at lower values of CTOD than for higher aspect ratio cracks or defects. While the concept of constraint influence on toughness is well known, none of the methodologies available to predict fracture conditions for girth welds containing defects includes this constraint influence. Second, the safety margin appears to increase rapidly with failure strain above the yield level. This is presumably because the NBS model predicts that CTOD will grow without bound as the applied strain approaches yield strain: an inherent consequence of its elastic-perfectly plastic material model.

6. ASSESSMENT OF PROPOSED DEFECT TOLERANCE CRITERIA

Of the five defect tolerance criteria assessed here, three (the appendices of BS 4515, **CSA** 2184, and **API** 1104) have been proposed as specific standards for determining which girth weld defects require repair. The basis on which these defect tolerance criteria should be evaluated include:

- Their ability to produce consistently conservative allowable defect dimensions.
- The avoidance of excessively conservative and costly limitations.
- The existence of the capabilities (e.g., inspection) which are required to utilize the criterion.
- The consistency of the criterion with other related standards and regulations.
- The lack of ambiguity of the criterion.
- The appropriate level of sophistication such that the criterion is readily usable by the appropriate professional staff, i.e., design engineers and field inspectors.
- The ability to subsequently verify that the criterion was properly utilized.

The ability of a proposed girth weld defect tolerance standard to produce consistently conservative allowable defect dimensions without imposing excessive restrictions depends on the input requirements (material properties, defect sizing, and service load conditions) and on the methodology for obtaining results from the input, e.g., COD Design Curve, plastic collapse criterion, etc. The proposed standards all require that toughness be measured as specified in BS **5762.** They have

different approaches to defect sizing, service loads, and calculation of allowable defect sizes in terms of the material properties and loading conditions. We will use the information on service loads (Section 2), the results of the comparative calculations for the representative examples (Section *3),* and the results of the application of the methodologies (representing the criteria) to the experimental data (Section 5) to evaluate the technical aspects of the proposed criteria. We will also co mment on the applicability of the proposed standards to actual pipeline assessments, addressing the extent to which they are explicit and unambiguous, usable by the appropriate staff, and subsequently verifiable. It is anticipated that pipeline designers will perform the calculations to set allowable defect dimensions at the time of the pipeline design and that field inspectors will use the results to make defect repair decisions. The calculation of allowable defect sizes should give generic results independent of the analyst and the results should be in a form which can be effectively utilized in the field by the inspector.

The PD *6493,* while not a proposed girth weld defect tolerance assessment criteria, is a detailed methodology for determining allowable defect sizes in weldments. It requires that the user input information on toughness and loading or defect size, resulting in corresponding estimates of allowable defect dimensions or applied stresses. The PD *6493* includes elastic crack geometry and residual stress corrections to the COD Design Curve as well as a plastic collapse limitation on defect size or applies stress. It results in conservative estimates of allowable strain or allowable defect dimensions for all cases considered. The degree of conservatism is not uniform and in numerous cases may be excessive.

The BS *4515* Appendix H is based on PD *6493;* however, the applied stress is limited to the yield stress, and the defect (cracks are not permitted) is taken as having a depth of 3 mm (assumed to represent one weld pass). The use of BS *4515* Appendix H results in a required material toughness which depends only on the pipe diameter, thickness and yield strength. For pipelines which meet this requirement, defect

length is limited based on pipe diameter. Application of the Methodology 3 on which BS 4515 Appendix H is based resulted in conservative estimates for failure strain in all cases considered. BS 4515 Appendix H can currently be applied with no reduction of pipeline integrity or safety provided there is assurance that the actual defects are limited to a 3 mm depth as assumed in the analysis which supports this standard; however, application of this standard may result in overly conservative defect removal decisions.

The CSA 2184 Appendix K is similar to PD 6493 in that it requires user inputs of defect size or applied.stress and results in corresponding ranges of allowable stress level or defect dimensions. Application of CSA 2184 Appendix K to the data available in this study resulted in consistently conservative predictions for allowable strain levels. This standard is unique in that it does not require an absolute minimum toughness and does not include a residual stress correction. It is possible that this could lead to less conservative (or nonconservative) predictions for conditions not addressed here which involve lower toughness materials and/or high residual stresses.

The API 1104 Appendix A differs from the other defect tolerance criteria in that it does not adjust the COD Design Curve to account for crack geometry and does not include a plastic collapse-based limit on defect size or allowable load level. Application of the Methodology 1, on which the standard is based, to the available data resulted in a wide range of safety margins or failure strains and nonconservative predictions for allowable strains for some data points associated with long flaws. An earlier study by Wilkowski and Eiber came to a similar conclusion. [13] Comparison of Methodology 1 with the other methodologies considered indicates that the scatter in the safety margin can be reduced and the nonconservative predictions eliminated by including geometry corrections to the COD Design Curve and a plastic collapse based limit on applied stress.

The API 1104 Appendix A requires a minimum toughness of 0.005 inches at 15°C below the lowest operating temperature. This condition was not satisfied by the available experimental data. Thus no conclusion can be reached regarding the safety margin that would result from application of the proposed standard to test results involving higher toughness weldments.

The API 1104 Appendix A implicitly permits application to applied strain levels beyond yield--a range which is not allowed by the pipeline standard ANSI/ASME B31.8. The higher strain range is apparently permitted in order that the standard may also be applied to pipeline installation conditions, a situation not treated in the present study. Neither the API 1104 Appendix A nor the other proposed standards reviewed here account for possible residual stresses or stable tearing which could result from large installation strains.

The API 1104 Appendix A requires field measurement of defect length and depth dimensions. While nondestructive evaluation was not the focus of the present study, the concern is raised that tools for performing these measurements with appropriate accuracy and confidence may not be available, and therefore, may prevent effective application of this proposed standard.

We recommend that API 1104 Appendix A be altered in *two* areas prior to usage as a girth weld defect tolerance standard for pipeline service conditions. First, it should be made consistent with the base standard on the topic of allowable longitudinal pipeline stresses. In addition, the standard should be altered (or new data provided) to address the apparent lack of conservatism in its application to the long flaw problem. Possible approaches for altering the standard in this area include, but are not limited to, further restriction on allowable defect length, inclusion of a plastic collapse limit, and/or inclusion of a crack geometry correction to the COD Design Curve.

The NBS procedure is based on **LEFM** using the Irwin model for ligament yielding associated with surface cracks.and the Dugdale model to account for yielding beyond the crack length. It includes a residual stress correction. Based on an elastic-perfectly-plastic material model, it does not allow the applied stress to exceed the material flow stress. No explicit safety margin is currently built into the NBS procedure, though one could certainly be added. The failure strain predictions based on the NBS methodology did not correlate closely with the observed failure strains. There appears to be a crack geometry aspect ratio (a/ℓ) influence on the ratio of predicted to measured failure strain. This effect could be the result of constraint influences on critical crack tip opening displacement and/or on the amount of stable tearing which precedes failure. Neither of these influences are accounted for by the NBS model. The NBS methodology follows a procedure developed to determine the conditions for crack growth initiation rather than final failure; however, it is applied in conjunction with failure crack tip opening displacement data. The ambiguity in the NBS method with respect to crack growth initiation and failure predictions may be a cause for the disparity between its predictions and observations.

The NBS criterion for setting allowed defect sizes is based on a more substantial theoretical foundation than the other approaches which were reviewed here. The NBS methodology involves calculation of the crack tip opening displacement in terms of geometry, material properties, and loading conditions. Conversely, the PD 6493, BS 4515 Appendix HCSA 2184 Appendix K, and API 1104 Appendix A are each based on the COD Design Curve with various corrections. Our observations indicate that, in spite of this distinction, the NBS methodology does not necessarily produce better estimates of allowable strain level or defect size than the best of the empirical methods. The reason for this may be that when a theoretical model is utilized it is necessary to explicitly account for all the factors which influence failure conditions. In this case these factors include above yield material hardening, stable tearing, and the influence of geometry on apparent material toughness.

7. SUMMARY AND RECOMMENDATIONS

There is currently no methodology which is able to accurately predict failure--leak or break--of pipeline girth welds. Two approaches have been reviewed here. The first, based on the COD Design Curve, is empirical and can be made to be conservative by including adjustments for crack geometry, residual stress, and plastic collapse. The alternative approach typified by the NBS procedure is based on correlation of failure conditions with values of a crack tip parameter, e.g., the crack tip opening displacement. Each approach has merit and application and each can be improved from its present implementation by further research efforts.

Methods have been developed to include the influence of crack or defect geometry, residual stress, and plastic collapse when applying the COD Design Curve methodology. Each of these factors has been shown to be important and their influence must be accounted for to obtain reliably conservative allowable strains. However, the models for each of these influences could potentially be improved and these improvements would lead to more consistent allowable strain estimates.

The crack geometry influence is generally treated using elastic analysis results for surface defects. Results presented earlier demonstrate that this approach does not completely account for crack geometry effects. This is expected because the stress states considered are elastic-plastic rather than elastic. The Canadians, recognizing this, have proposed to correct the analytical results based on this experimental observation. We have shown by example in Appendix B that elastic-plastic geometry corrections can be more substantial than those predicted based on elastic solutions. Thus, the magnitude of geometry correction depends on the level of stress as well as the defect geometry. The development of crack geometry adjustments including plastic effects would improve the ability of the COD Design Curve to provide estimates for allowable strain with consistent safety margins.

We would recommend that research continue in attempt to develop better theoretical models for the prediction of failure conditions for girth welds containing defects and that the results of the research be made available to aid in improvement of girth weld defect tolerance standards. However, at the present, it appears that such standards should be based on the COD Design Curves with appropriate corrections to account for the various influences discussed above.

In a similar manner, it is recognized that residual stresses influence the applied strain at which crack growth occurs, but the current procedure for adjusting for residual stress does not take into account the amount of plastic deformation at fracture. The development of an approach for improving residual stress corrections to address this would lead to improved COD Design Curve allowable strain estimates.

Similarly, it is recognized that failure can precede COD Design Curve estimates if full yielding of the section occurs. An approach which would enable accurate (rather than conservative) predictions of plastic collapse would also contribute to enhanced accuracy of the COD Design Curve methodology.

With respect to methodologies which are based on a crack tip parameter such as CTOD, the available approaches are each lacking in some aspect. The NBS approach makes use of elastic-perfectly plastic material models and, therefore, is unable to deal with the full plastic regime. The Elastic-Plastic Estimation Procedure which does account for material hardening still requires the development of solutions for relevant crack and pipe geometries. Research would be properly directed toward developing tools which can handle both material hardening and surface defects. Even if such solutions become available, research is required to tackle the more fundamental problem of constraint and its influence on crack growth conditions.

REFERENCES

1. "Minimum Federal Safety Standards for Liquid Pipeline," Code of Federal Regulations, Title 49 Transportation, Part 192 and 195, Office of the Federal Register, National Archives and Records Service, General Services Administration (revised 1 Oct. 1975).

2. API 1104, Standard for Welding Pipelines and Related Facilities, fifteenth edition, American Petroleum Institute, Washington, D.C., 1980.

3. Fracture Mechanics Study of Buried Field Girth Welds, Alyeska Pipeline Service Company, July 1976.

4. "Consideration of Fracture Mechanics Analysis and Defect Dimension Measurement Assessment for the Trans-Alaska Oil Pipeline Girth Welds," NBSIR 76-1154, National Bureau of Standards, Gaithersburg, Maryland, Oct. 1976.

5. PD 6493:1980, "Guidance on Some Methods for the Deviation of Acceptance Levels for Defects in Fusion Welded Joints," British Standards Institution, 1980

6. BS 4515, "Specifications for Field Welding of Carbon Steel Pipelines," British Standards Institution, London, 1969.

7. BS 4515 Appendix H, "A Proposed Appendix for BS 4515 Containing Defect Tolerance Criteria for Girth Welds Based on Fracture Mechanics Approach," British Standards Institution, London, 1982.

8. API 1104, Sixteenth Edition, Appendix A, "Alternative Standards of Acceptability for Girth Welds," American Petroleum Institute, 1983.

9. CSA 2184 Appendix K Draft, "Proposed Changes to CSA A184 to Accommodate Alternative Standards of Acceptability," Canadian Standards Association, Toronto, Canada, 1984.

10. CSA Z184-M 1983, "Gas Pipeline Systems," Canadian Standards Association, Toronto, Canada, 1983.

11. "Fitness-for-Service Criteria for Pipeline Girth Weld Quality," Final Report, Fracture and Deformation Division, National Bureau of Standards, Boulder, CO, Nov. 1, 1983.

12. Kumar, V., German, M.D. and Shih, C.F., "An Engineering Approach for Elastic-Plastic Fracture Analysis," Rep. NP-1931, Electric Power Research Inst., Palo Alto, CA, 1981.

13. Wilkowski, G.M. and Eiber, R.J., "Evaluation of the Inherent Safety Factors in the Tentative API Girth Weld Defect Tolerance Approach," AGA Catalog No. L-51385, 1979.

14. ANSI/ASME B31.8, "Gas Transmission and Distribution Piping Systems," American Society of Mechanical Engineers, 1983.

15. "Summary Report - Design Criteria and Stress Analysis for the Trans-Alaska Pipeline," Alyeska Pipeline Service Company, 1973.

16. Erdogan, F., Theoretical and Experimental Study of Fracture in Pipelines Containing Circumferencial Flaws," Report DOT-RC-82007, Lehigh U., August 1982.

17. Wilkowski, G.M. and Eiber, R.J., "Review of Fracture Mechanics Approaches to Defining Critical Size Girth Weld Discontinuities," Weld. Res. Council Bull. 239, July 1978.

18. Dawes, M.G. and Karnath, M.S., "The Crack Opening Displacement (COD) Design Curve Approach to Crack Tolerance," Conference on the Significance of Flaws in Pressurized Components, Institution of Mechanical Engineers, London, England, May 1978.

19. BS5762:1979, "Methods for Crack Opening Displacement (COD) Testing," British Standards Institution, London, 1979

20. Willoughby, A.A. and Garwood, S.J., "The Application of Maximum Load Toughness to the Defect Assessment in a Ductile Pipeline Steel," presented at the Sixteenth ASTM Symposium on Fracture Mechanics, Columbus, OH, 15-17 August 1983.

21. Reed, R.P., Kasen, M.B., McHenry, H.I., Fortunko, C.M. and Read, D.T., "Fitness-for-Service Criteria for Pipeline Girth-Weld Quality," Welding Res. Council Bulletin 296, July 1984.

22. Wilkowski, G.M. and Eiber, R.J., "Evaluation of Tensile Failure of Girth Weld Repair Grooves in Pipe Subjected to Offshore Laying Stresses," J. Energy Resources Tech, Trans ASME, 103, March 1981, pp. 48-55.

23. Duffy, A.R., Eiber, F.J. and Maxey, W.A., "Recent Work on Flaw Behavior in Pressure Vessels," Proc. Symp. on Fracture Toughness Concepts for Weldable Structural Steel, Risely, England, April 1969, UKAEA.

24. Eiber, R.J., Maxey and Duffey, "Investigation of the Initiation and Extent of Ductile Pipe Rupture," Battelle Memorial Institute Report 1908, 1971.

25. Glover, A.G., Coote, R.I. and Pick, R.J., "Engineering Critical Assessment of Pipeline Girth Welds," presented at Fitness for Purpose Validation of Welded Constructions, London, 17-19 Nov. 1981.

26. Glover, A.G. and Coote, R.I., "Full-Scale Fracture Tests of Pipeline Girth Welds," presented at Fourth Nat. Congress on Pressure Vessels and Piping Technology, Portland, OR, 19-24 June 1983.

27. Glover, A.G., "Effects of Real Defects on Girth Weld Fracture Behavior," AGA Report Catalog No. L51457, American Gas Association or Welding Institute of Canada, Rep. RC75/3/83, Jan. 1984.

28. Hopkins, P., Jones, D.G. and Fearnehough, G.D., "Defect Tolerance in Pipeline Girth Welds," presented at Fourth Nat. Congress on Pressure Vessel and Piping Technology, Portland, OR, 19-24 June 1983.

29. Erdogan, F., "Theoretical and Experimental Study of Fracture in Pipelines Containing Circumferential Flaws," Lehigh U. Report to the Dept. of Transportation, Contract DOT-RC-82007, Sept. 1982.

30. Kanninen, M.F., et al., "Instability Predictions for Circumferentially Cracked Type-304 Stainless Steel Pipes Under Dynamic Loading-Volume 1," Electric Power Research Inst., Report EPRI NP-2347, April 1982.

31. German, M.D., et al., "Elastic-Plastic Fracture Analysis of Flawed Stainless Steel Pipes," Electric Power Research Inst. Report EPRI NP-2608-LD, Sept. 1982.

32. "Pipeline Accident Report - Michigan - Wisconsin Pipe Line Company, Gas Transmission Line Failure, South of Monroe, Louisiana," National Transportation Safety Board, NTIS Report PB-241 988, April 1975.

33. Picklesimer, M.L., "Examination of Fractured Weld in 16 Inch Steel Pipe Gas Main, Philadelphia Electric Company, West Conshohocken, Pennsylvania," National Bureau of Standards, NTIS Report PB-243 532, Aug. 1971.

34. Picklesimer, M.L. and Shives, T.R., "Examination of Failed Eight Inch Welded Steel Pipe Natural Gas Main, UGI Corp., Coopersburg, Pennsylvania," National Bureau of Standards, NTIS Report PB-243 543 Nov. 1973.

APPENDIX A

A DESCRIPTION OF THE FRACTURE MECHANICS ASPECTS OF API 1104 APPENDIX A

The purpose of API 1104 Appendix A is to set allowable defect sizes in pipeline girth welds and to specify conditions on welding, fatigue, environment and toughness under which such an assessment can be made. A description of some of the aspects of API 1104 Appendix A can also be found in reference [A1]. The criterion for determining acceptable defect depths is the COD-Design Curve, which is used in the form

$$a = \frac{\delta}{2\pi(e_t - 0.25e_o)} \qquad \text{(A1)}$$

where

a = the maximum depth of a surface defect or one-half the maximum height of a buried defect

δ = the critical crack tip opening displacement determined from three-point bend tests

e_t = the total applied strain

e_o = the yield strain

The total applied strain is the sum of the applied strain--as determined from stress analysis--and a residual strain equal to the yield strain. In API 1104 Appendix A, e_o = 0.2 percent.

The allowable initial defect depth, which is the defect depth measured immediately after pipeline construction, is actually smaller than predicted by equation A1 in order to account for fatigue propagation of the defect during the life of the pipeline. Fatigue

crack propagation is calculated using linear elastic fracture mechanics (LEFM) and the power law relation

$$da/dN = A\,(\Delta K)^m$$

where

N - number of cycles

A,m - empirical constants from laboratory data; in the derivation of API 1104 Appendix A, $A = 3.6 \times 10^{-10}$ and $m = 3.0$ (units in ksi$\sqrt{in}$ and inches/cycle).

ΔK - $M(\Delta\sigma)\sqrt{\pi a}$; stress intensity factor range

$\Delta\sigma$ - stress

M - a geometry factor

The factor M can be written

$$M = \left(\frac{M_s M_t}{\phi}\right)(M_w)\sqrt{\pi} \qquad \text{(A2)}$$

The first three parameters are correction factors for crack geometry: M_s and ϕ - crack shape, M_t - thickness. The values of these parameters are taken from Maddox. [A2] M_w is apparently an empirical factor for curvature and flaw length obtained from pipe fracture tests. [A3]

$$M_w = \frac{1-a/tM_c}{1-a/t}, \quad M_c = \left[1 + 0.26\alpha + 47\alpha^2 - 59\alpha^3\right]^{1/2} \qquad \text{(A3)}$$

where

α = $\ell/\pi D$

ℓ = defect length

D = pipe diameter

The factor a is the ratio of flaw length to circumference. A value of M = 2.85 was used in the derivation of API 1104 Appendix A. This value is greater than values calculated from equation A2 for all of the allowable defect geometries of the Appendix. The choice that M be less than 2.85 is apparently part of the basis for choosing the requirement that $\ell \leq 4t$ for $0.25 \leq a/t < 0.5$. Furthermore, the requirement that $M \leq 2.85$ seems to be the basis for Figure A7 in Appendix A, which sets limits on the flaw length for $D/t < 17$ and API 1104 $0.25 \leq a/t < 0.5$.

We note that the correction factors for buried defects are always less than those for surface defects with the same a and 2c dimensions.

Given the value of M, the fatigue crack growth equation is integrated to calculate the maximum initial crack depth. A simplified integration, which does not account for load sequence effects or crack geometry changes, is used in the derivation of Appendix A. The result is

$$a^* = \left(a_f^{-\frac{1}{2}} + 4.17 \times 10^{-9} S^* \right)^{-2}$$

where

a^* = allowable initial crack depth

a_f = allowable final crack depth, from equation (Al)

$$S^* = \sum_{i=1}^{k} (\Delta\sigma_i)^3 N_i = 4 \times 10^7 \ (\text{ksi})^3$$

The value of S* was chosen to represent a severe pipeline fatigue history. Table A1 shows the number of cycles required to make $S^* = 4 \times 10^7 (ksi)^3$ for various levels of constant alternating stress.

Table A1 Number of Cycles Reauired for $S^* = 4 \times 10^7 (ksi)^3$

$\Delta\sigma$(ksi)	N
5	320,000
10	40,000
15	12,000
20	5,000
30	1,500

If the calculated value of S* for the pipeline in question is greater than $4 \times 10^7 (ksi)^3$, Appendix A cannot be used to assess allowable defect sizes.

The final integrated fatigue equation is

$$a^* = \left(a_f^{-\frac{1}{2}} + 0.1667\right)^{-2} \qquad (A4)$$

Equations A1 and A4 were used to generate Figure A5 of API 1104 Appendix A, which is the curve that defines maximum allowable initial crack depths.

Only two curves for allowable crack depth are given in Figure A5. These correspond to two levels of fracture toughness: $\delta = 0.005$ in. and $\delta = 0.010$ in. There is no interpolation for other values of toughness. Appendix A requires that $\delta = 0.005$ in. be used if the measured toughness is between 0.005 in. and 0.010 in., and that $\delta = 0.010$ in. be used if the measured toughness equals or exceeds 0.010 in. Also, the material toughness must be measured at 15°C below the anticipated service

temperature. If $\delta < 0.005$ in., Appendix A cannot be used. A minimum value of fracture toughness equal to 0.005 in. and determined at 15°C below the lowest anticipated service temperature was chosen in an effort to ensure that the material is at or close to its upper shelf fracture behavior when in service. The upper limit set on toughness is in recognition of the limited toughness measuring capacity of the necessarily small test specimens from pipelines.

Example 1: Maximum Allowable Defect Depth for Figure A5 of API 1104 Appendix A

δ = 0.005in., applied strain e_a = 0.2% (0.002)

$$a_f = \frac{0.005}{2\pi\ (0.002 + 0.002) - 0.25\ (0.002)} = 0.227 \text{ in.}$$

$$a^* = \left[(0.227)^{-1/2} + 0.16671\right]^{-2} = 0.195 \text{ in.}$$

Example 2: Maximum Allowable Defect Length for 3<D/t<17, 0.25<a/t<0.50 for Figure A7 of API 1104 Appendix A.

M = 2.85

D/t = 10

a/t = 0.50

The value of ℓ/t must be solved for iteratively:

a/ℓ	$\ell/\pi D$	M_w	$\frac{M_s M_t}{\Phi}$	M
0.10	0.16	1.29	2.78	3.59
0.20	0.08	1.12	2.05	2.30
0.15	0.11	1.19	2.42	2.88

Actually, a/ℓ = 0.145 gives M = 2.85 and $\ell/t = (a/t)/(a/\ell)$ = 3.45.

REFERENCES

A1. Von Rosenberg, E.L. and Royer, C.P., "Pipeline Welding Standards," Presented at the Amer. Welding Soc. Conf., Houston, Texas, 1982.

A2. Maddox, S.J., "An Analysis of Fatigue Cracks in Fillet Welded Joints," Int. Journ. of Fracture, 11 (1975) 221-243.

A3. Wilkowski, G.M. and Eiber, R.J., "Evaluation of Tensile Failure of Girth Weld Repair Grooves in Pipe Subjected to Offshore Laying Stresses," Transactions of the ASME, Journal of Energy Resources Technology, Vol. 103, March 1981.

APPENDIX B

A STUDY OF PLASTICITY EFFECTS ON THE CRACK GEOMETRY CORRECTION FACTORS USED WITH THE COD-DESIGN CURVE

The COD Design Curve is a semi-empirical approach for determining allowable defect sizes and applied stresses and strains for engineering structures. As originally conceived, the Design Curve applied to wide plates containing small through cracks and loaded in remote tension (c.f[B1]); the fundamental aspects of the Design Curve are based on this geometry. The COD Design Curve, because of its derivation and based on experience, has been found to have a factor of safety of approximately two. Applications of the Design Curve, carried out mainly through the British PD 6493 now include edge cracks in wide plates and surface and buried defects. The half crack length, $\bar{a}$, used in the COD Design Curve is equated to the crack depth for surface cracks and to one-half the crack height for buried defects. Such applications of the Design Curve for these defect geometries seem logical when sections of the surface and buried defects are considered, as in Figure B1.

It was recognized in applying the COD Design Curve to geometries other than the wide plate, that some correction was needed to account for the crack shape and the proximity of the crack tip to the front and back surfaces. The corrections used in the British document PD6943 are based on linear elastic fracture mechanics (LEFM). Given the geometry of the defect and the thickness of the structure, one finds the crack length for the infinite plate containing a through crack which will give the same crack tip opening displacement as the crack in the structure of interest. This procedure retains the same factor of safety that is in the basic COD Design Curve provided the structure is elastic. In the presence of plastic deformation it is not clear how the use of corrections based on linear elasticity will affect the factor of safety.

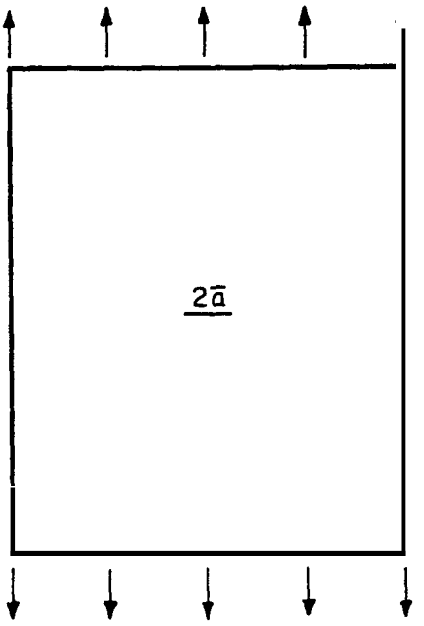

WIDE PLATE **WITH** THROUGH CRACK

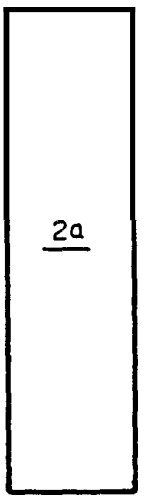

BURIED DEFECT SECTION

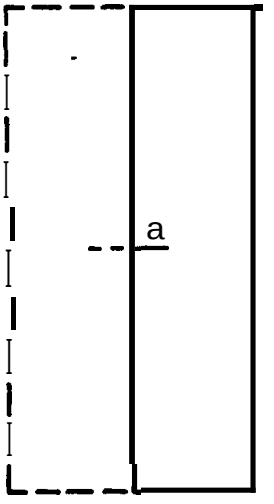

SURFACE DEFECT SECTION

Figure B.1 Comparison of the Sections of Buried and Surface Defects to the Wide Panel with a Through Crack

Recently, in applying the COD Design Curve to pipeline girth welds, Glover and Coote [B2] found that the factor of safety was nonuniform with respect to defect aspect ratio; the factor was smaller for crack length-to-depth ratios near zero. They recommended that the correction factors be changed so that a factor of safety of two would be retained for these long defects.

Failure strains in the tests considered by Glover and Coote exceeded 80% of the yield strain, indicating that plasticity effects may have contributed to the nonuniformity of safety factor in applying elastic correction factors to the data. In addition, fracture generally occurred by ductile tearing, sometimes in the regime of applied strain and stress for which plastic collapse is a better description of fracture.

This appendix presents an analysis of the effects of plasticity on the crack geometry correction factors used with the COD Design Curve. We will show, using the elastic-plastic estimation approach [B3], that the nonuniform safety factor with defect aspect ratio observed by Glover and Coote can be explained by plasticity effects. We do not maintain that this is the only cause.

COD Design Curve

The COD Design Curve is given by:

$$\delta = 2ne_o\bar{a} \begin{cases} (e/e_o)^2; & e/e_o \leq 0.5 \\ e/e_o - 0.25; & e/e_o \geq 0.5 \end{cases} \qquad \text{(B1)}$$

where δ = CTOD toughness
e_o = yield strain
e = applied strain
$\bar{a}$ = equivalent half crack length.

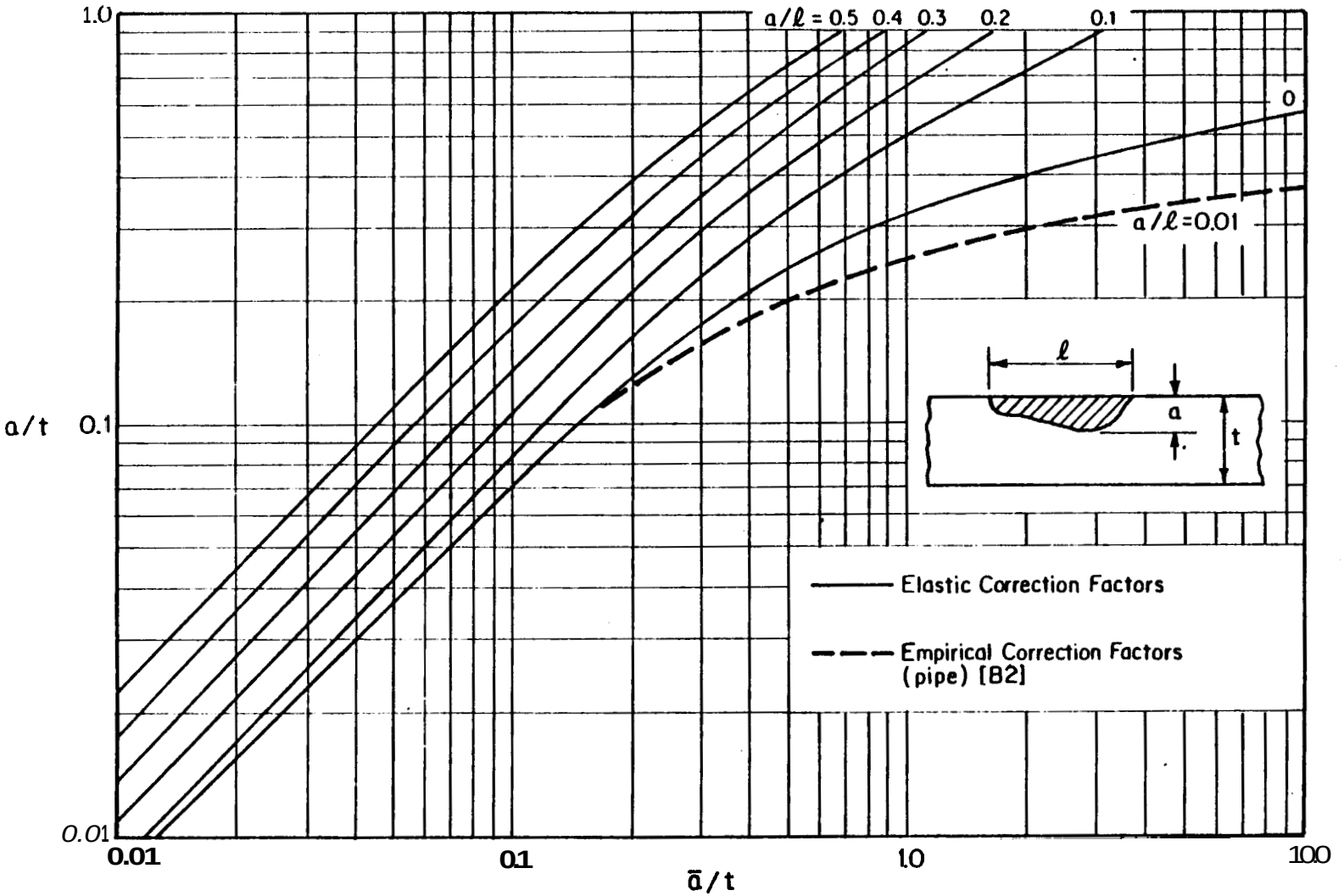

Figure B.2 Suggested Modification to the Crack Geometry Corrections of PD 6493 [B2]

The value of $\bar{a}$ is obtained by equating the elastic crack tip opening displacement (CTOD) for the crack geometry of interest to the CTOD for a through crack in an infinite plate under uniform tension; this is equivalent to equating the linear elastic stress intensity factors. Thus, we have

$$\sigma\sqrt{\pi\,\bar{a}} = M\sigma\sqrt{\pi\,a},$$

$$\bar{a} = M^2 a,$$

and normalizing by the plate thickness,

$$\frac{\bar{a}}{t} = M^2\,\frac{a}{t} \qquad \text{(B2)}$$

Values of M are obtained from analyses similar to that of Newman and Raju [B4]. The resulting correction factors, for surface defects, are shown graphically in Figure B2 as they appear in PD 6493. The curve for $a/\ell = 0$ corresponds to the single edge notched specimen in tension. We note that for deep relatively long defects the equivalent crack length, $\bar{a}$, can be larger than the plate thickness. Also shown in Figure 2 are the modified correction curves suggested by Glover and Coote. The modifications apply only for relatively long defects; there are no suggested modifications for $a/\ell \geq 0.1$.

Analysis for Long Defects

Calculation of correction factors that include the effects of plastic deformation requires elastic-plastic CTOD solutions for the geometry of interest -- in this case, surface defects in plates -- and the center cracked plate in tension. The elastic-plastic estimation approach is used for this purpose.

The elastic-plastic estimation procedure separates the CTOD, and other crack parameters, into elastic and plastic components. The elastic

component is calculated using LEFM with an Irwin plastic zone correction. The plastic component is obtained from detailed finite element calculations. Elastic solutions are available for many geometries, but the fully plastic solutions are tabulated for only a limited set of geometries [B3]. These include, among others, the center cracked panel (CCP), the single edge notched (SEN) specimen, and the hollow cylinder containing an internal, full circumferential crack, all loaded in tension.

The CCP solutions can be used to investigate the factor of safety on the COD Design Curve. We use for this purpose the elastic-plastic estimation formula for a crack length-to-width ratio of 0.125 to model an infinite plate: this is the smallest a/W ratio tabulated in the handbook.

The value of the CTOD given by the elastic-plastic estimation formula is

$$\delta = \delta_e + \delta_p = f(a_e)\,\frac{P^2}{E'\sigma_o} + \alpha e_o a h\left(\frac{a}{W}, n\right)\left(\frac{P}{P_o}\right)^{n+1} \qquad \text{(B3)}$$

where
- f = function of crack and component geometry
- a_e = plastically adjusted crack length
- E' = Young's modulus; $E' = E$ for plane stress, $E' = E/(1-\nu^2)$ for plane strain; ν = Poisson's ratio
- σ_o = yield strength; $\sigma_o = E e_o$
- P = applied load
- P_o = reference load; approximately the plastic limit load
- h = function of crack geometry and hardening exponent n
- W = component width

The values of a and n describe the stress-strain relation for the material according to

$$\frac{e}{e_o} = \frac{\sigma}{\sigma_o} + \alpha\left(\frac{\sigma}{\sigma}\right)^n. \qquad \text{(B4)}$$

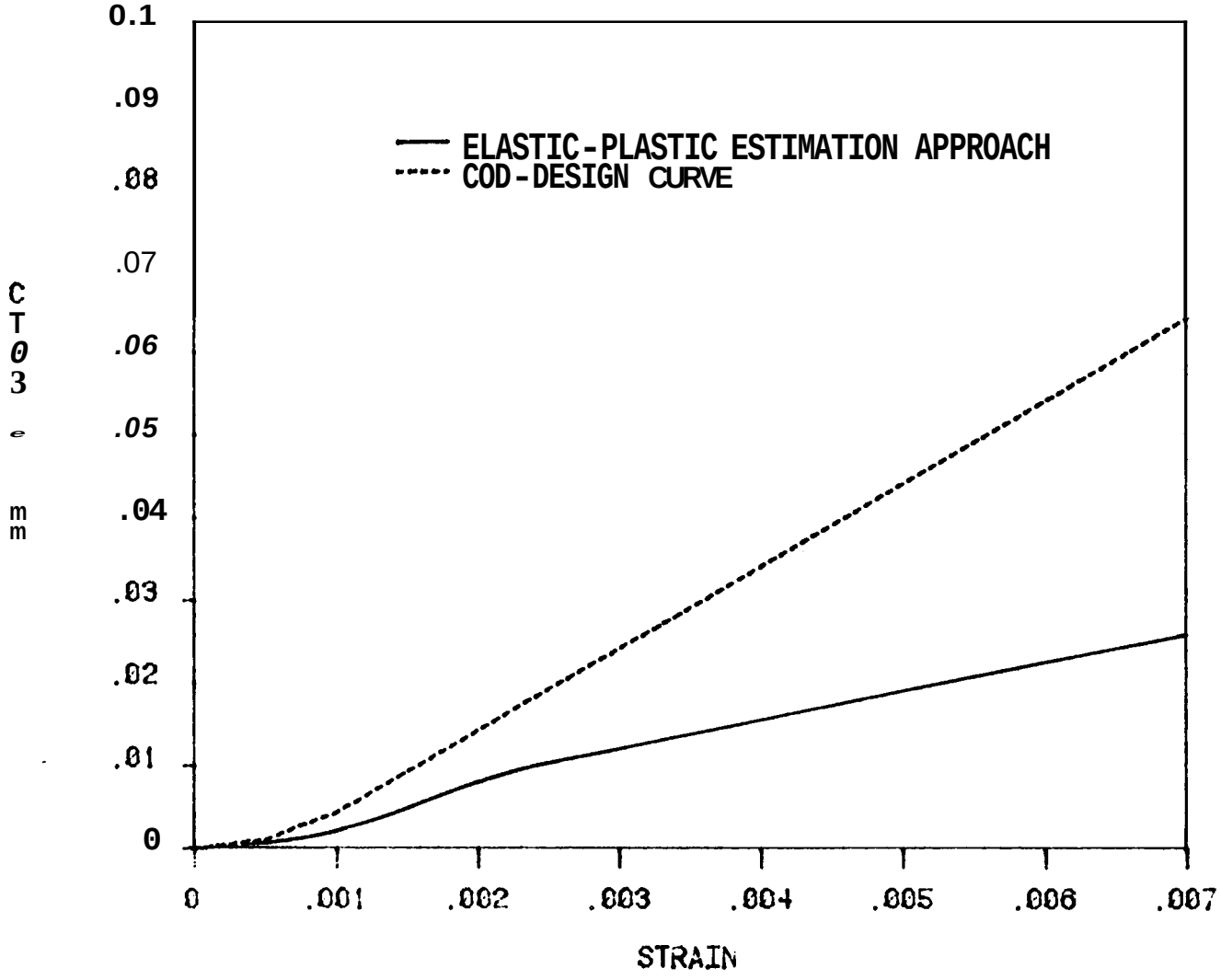

Figure B.3 Comparison of Calculated CTOD from the COD Design Curve to the CTOD from the Elastic-Plastic Estimation Approach, for a Center Cracked Panel; W = 1.0, a/W - 0.125

For a pipeline steel base metal with σ_o = 469 MPa (68 ksi) we find that a = 1.55, n = 20 [B5]. Figure B3 shows a plot of equations (B1) and (B3) for a material with : σ_o = 469 MPa (68 ksi), E = 207 x 10^3 MPa (30 x 10^6 psi), α = 1.55, n = 20, a/W = 0.125 and a = $\bar{a}$ = 3.18mm (0.125 in.). The COD Design Curve is seen to overestimate the CTOD by a factor of about two for the range of strains shown.

The single edge notched panel geometry is used to study the effect of crack depth on the COD Design Curve correction factors in the presence of plasticity. This geometry is equivalent to a surface crack with a/ℓ = 0, a > 0. Recall that the elastic SEN solution is the one used to generate the correction curve in Figure B2 for a/ℓ = 0. The elastic-plastic estimation formula for this geometry is very similar to equation (B3). Figure B4 shows a plot of CTOD for the SEN geometry, normalized by the CTOD for the CCP geometry with a/W = 0.125 as a function of strain; as before, σ_o = 469 MPa (68 ksi), E = 207 x 10^3 MPa (30 x 10^6 psi), a = 1.55, n = 20. Curves are shown for two values of a/W for the SEN geometry.

Curves such as those shown in Figure B4 can be used to calculate crack geometry correction curves as in Figure B2 for various levels of strain. The elastic-plastic estimation equation (B3) can be written as the product of the crack length times a function of the ratio a/W for the different geometries under consideration here [B6]; that is,

$$\delta = a \quad F(a/W, \ldots).$$

Therefore, the crack length for the wide plate containing a small through crack--modeled by the CCP geometry with a/W = 0.125--required to give the same CTOD as the SEN geometry is given by

$$\bar{a} = a \frac{F_{SEN}(a/W)}{F_{CCP}(a/W=0.125)} \qquad (B5)$$

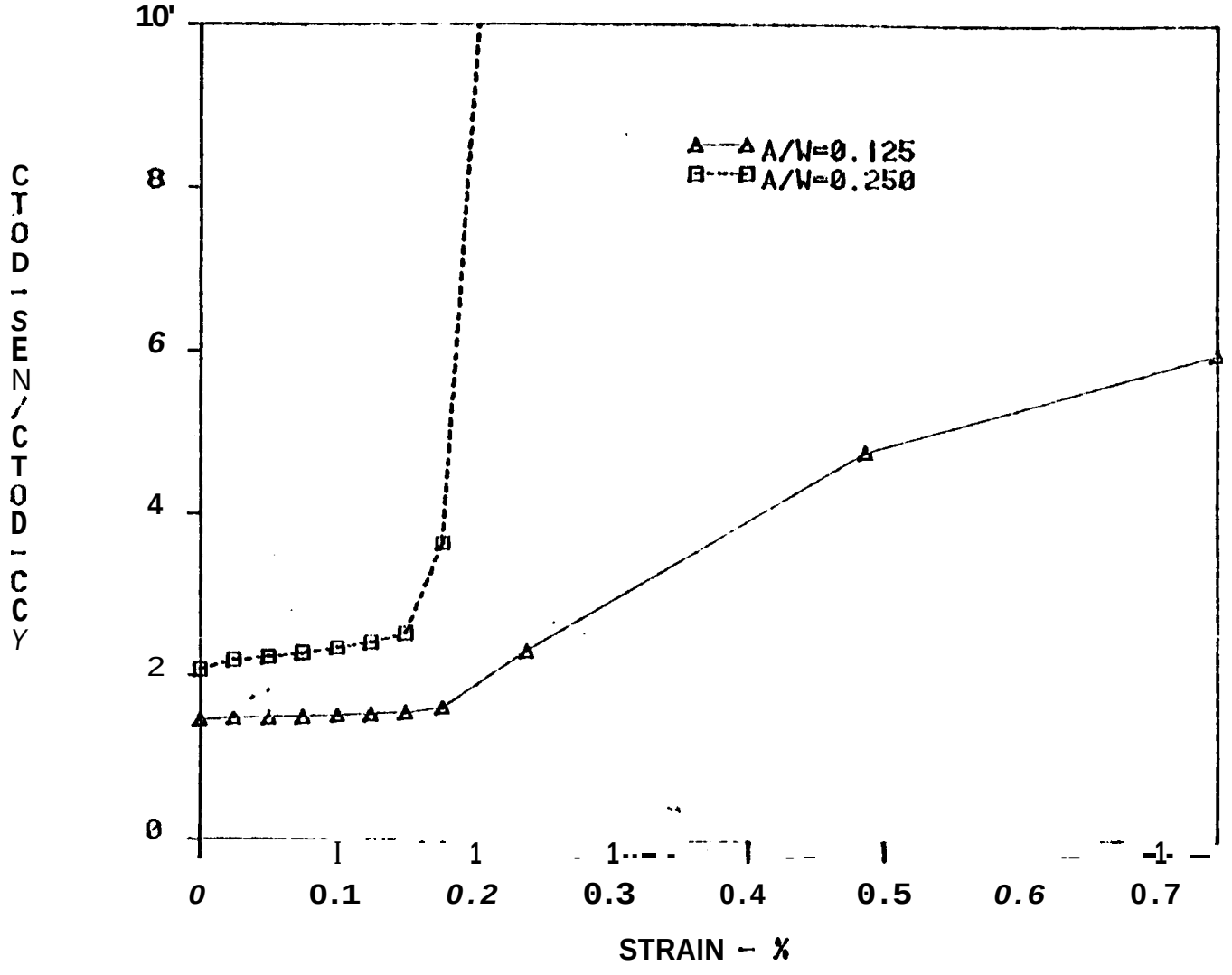

Figure 8.4 The Ratio of CTOD for the SEN Geometry to the CTOD for the CCP Geometry for Two Values of a/W but with Equal Crack Lengths

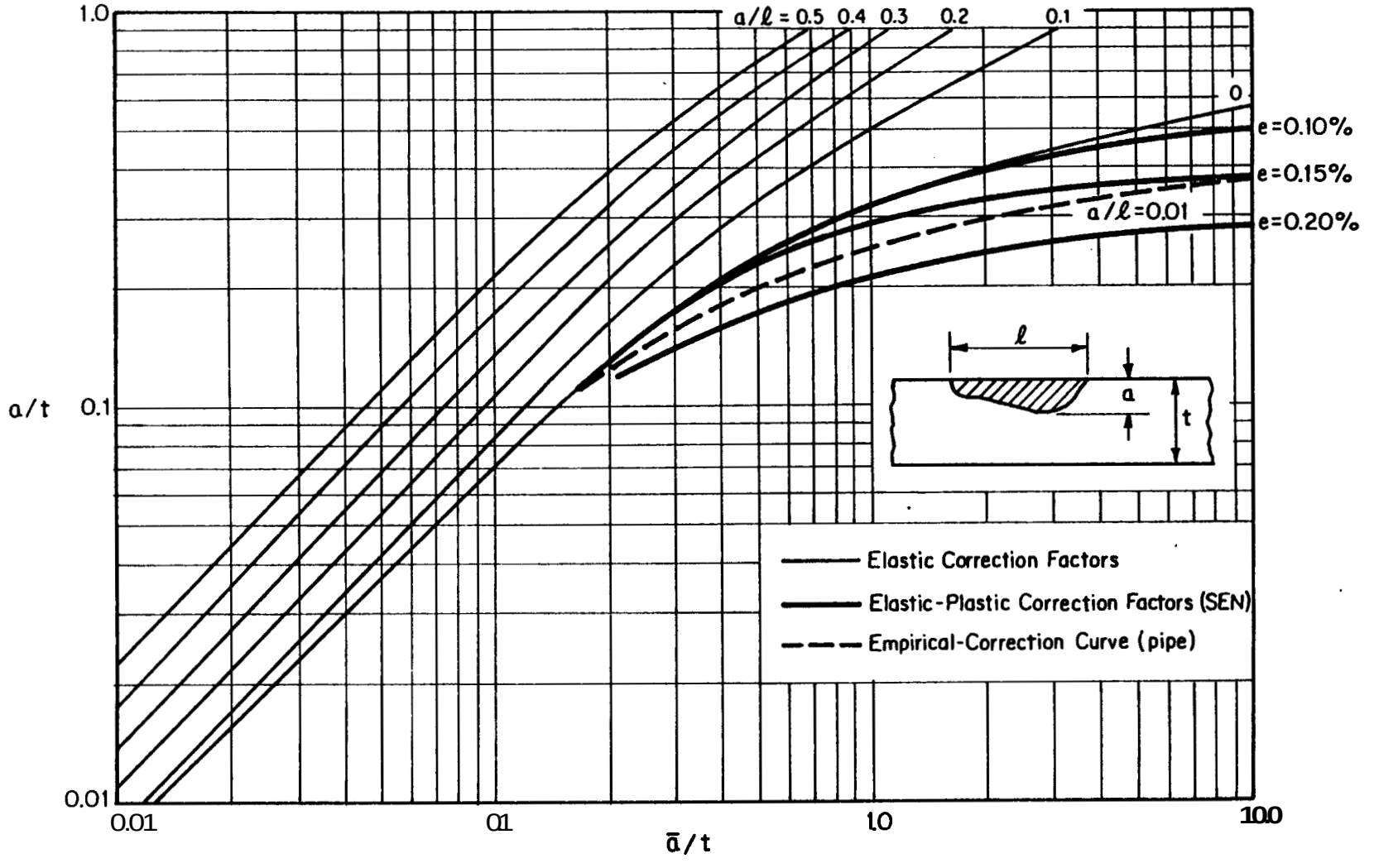

Figure B.5 **Geometry Correction Curves According to the Elastic-Plastic Estimation Approach for Three Stain Levels and in Comparison to the Elastic and Empirical Correction Curves**

This equation is equivalent to the elastic equation (B2). One can also see that the ratio of F factors on the right side of equation (B5) is the same ratio plotted on the ordinate of Figure B4; that is, it is also equal to the ratio of the CTOD values for equal crack lengths. Using data of the type shown in Figure B4 for various ratios of **a/W**, one can plot a curve of $\hat{a}/W$ vs. a/W similar to those shown in Figure B2 for various levels of strain, This has been done in Figure B5, but with W replaced by t to represent the plate thickness. The figure shows that for nominally elastic strains, e = 0.102, the curve follows the elastic curve, as it should, except for large values of a/t. At large values of a/t the SEN geometry is close to its plastic limit load so that, even though far field stresses are below yield, significant yielding is occurring in the cracked cross section. At higher levels of strain, the deviation of the plastic correction curves from the elastic correction curves occurs at lower crack depths. Also shown in Figure B5 is the shifted correction curve recommended by Glover and Coote for **a/ℓ** = 0.01.

Use of the SEN model to determine crack geometry correction factors for circumferential cracks in pipelines may not be approgriate. In an SEN specimen loaded in remote tension, some rotation will occur at the crack. This results in a larger CTOD than is expected in a pipe, since the pipe will tend to resist this rotation due to its cylindrical geometry. This can be investigated by calculating correction factors from solutions for the hollow cylinder containing an internal, complete circumferential crack. Elastic-plastic estimation formulas also exist for this geometry, but are tabulated only for hardening exponents of 10 and below. Figure B6 shows a plot of CTOD for the cylinder and SEN geometries normalized by the CTOD for the CCP geometry with a/W=0.125, as a function of strain; σ_o=469 MPa (68 ksi), E=207 x 10^3 MPa (30 x 10^6 psi), α= 1.0, n=10, R_i (internal radius)=254mm (10.0 in.), R_o (outer radius)=267mm (10.5 in.). The correction factors based on the cylinder geometry are not as great as those based on the SEN geometry.

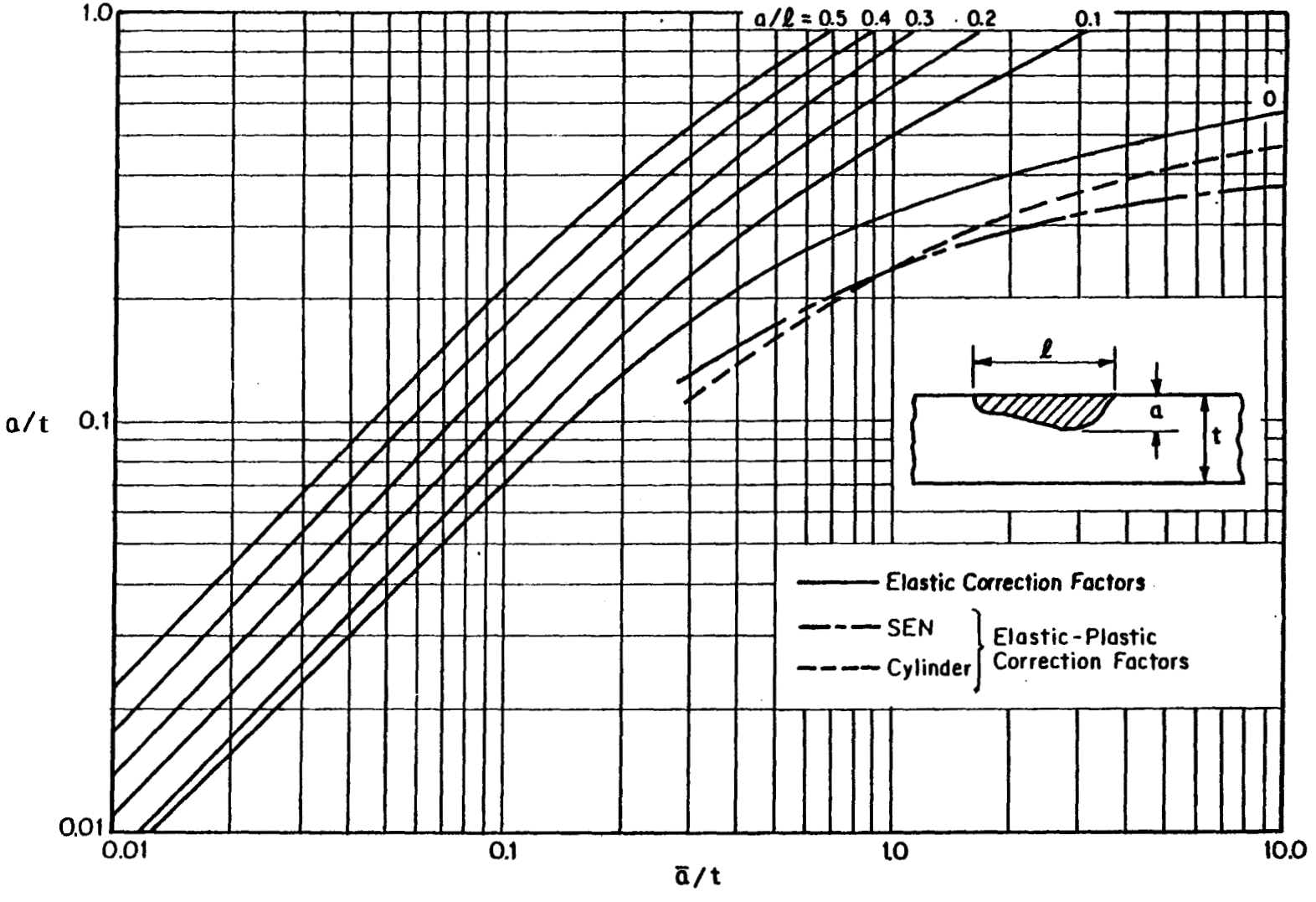

Figure B.6 Comparison of Elastic-Plastic Correction Factors Calculated Using the SEN and Cylinder Geometries

Short Defects

The analysis of the plasticity effects on geometry corrections for long surface flaws was possible because of the plain strain approximation via the SEN geometry. Shorter surface cracks cannot be analyzed as easily because there are currently no analytic or tabulated solutions which provide a method to calculate CTOD in the presence of plasticity for this geometry. Some numerical results are available and one set of these will be used to study the plasticity correction for short defects. Wilkening, deLorenzi and Barishpolsky [B7] have conducted three-dimensional elastic-plastic finite element analyses for axial surface cracks in a pressure vessel.' They considered a cylinder with internal radius R_i=2.3m (90in.) and wall thickness t=229mm (9in.), which gives R_o/R_i=1.10. Two defect depths and three defect aspect ratios were treated: a/t=0.25, 0.75 and ℓ/a=6,4, and 3. The internal pressures studied caused elastic stresses and stresses that exceeded the uniaxial yield strength, and crack face pressure was modeled. We consider here, only applied stresses below the yield strength.

Equation (B4) was used in [B7] to model the stress-strain behavior with: σ_o=414 MPa (60ksi), e_o-0.002, α=1.4 and n=8.6. A partial list of their results for CTOD and J at the deepest point in the crack are given in Table B1.

In order to estimate the geometry correction factors for these defects, calculations were made, as before, using the elastic-plastic estimation procedure with the center cracked panel geometry in plane strain tension and equation (B5), except with δ_{SEN} replaced by the CTOD values obtained by Wilkening, et al. [B7].

Table B1 Values of J and CTOD at the deepest crack extent for axial surface cracks in a pressure vessel [B7]; a/t=0.25 for all flaws; σ_o=414 MPa.

Internal Pressure (MPa)	a/ℓ	CTOD (mm)	J(kJ/m^2)	d=δ(σ_o/J)
17.2	0.167	0.045	32.5	0.57
	0.250	0.037	23.2	0.66
	0.333	0.030	18.3	0.68
31.0	0.167	0.171	129	0.55
	0.250	0.134	91	0.61
	0.333	0.109	70	0.64

Some difficulty arises in comparing CTOD values from a cylinder to a plate because of curvature effects and the variation of circumferential stress through the thickness. The average of the circumferential stresses at the inside and outside radii was used as input to the center cracked plate equations; the stresses at the inside and outside radii differ by about 10%. In addition, a stress equal to the internal pressure was added to the far field circumferential stress to account for crack face pressure.

The same material properties as used by Wilkening, et al. were used in the elastic-plastic estimation approach. The elastic-plastic estimation approach requires a value of d to calculate CTOD, where

For n=8.6 and in plane strain, it is recommended [B3] that d=0.63. However, as Table B1 shows, d varies from 0.51 to 0.68 for the particular range of conditions reported here. We have chosen a value of d=0.60 in calculating 6 for the center cracked panel geometry,

recognizing that we are studying plasticity effects as opposed to obtaining precise correction factors.

Table B2 shows the results of the calculated correction factors. The stresses corresponding to an internal pressure of 17.2 MPa are essentially elastic and the correction factors are seen to agree reasonably well with the correction factors currently used with the COD Design Curve which are based on linear elasticity. For the high pressure, or applied strain, the elastic-plastic correction factors are seen to decrease with respect to the elastic correction factors in contrast to the behavior for the long surface defects.

Discussion

Glover and Coote's observation of a nonuniform factor of safety with crack aspect ratio in the application of the COD Design Curve to pipeline girth weld defects can be explained by the results of our analysis. They found that the factor of safety for small defect aspect ratios -- short defects -- was three to five times that for large defect aspect ratios. Our results show that the correction factor for long defects should be greater and for short defects smaller or the same than those based on LEFM for strains on the order of the yield strain. Accounting for this difference would result in a more uniform factor of safety for the girth weld defect data.

There are other possible explanations for the observations of Glover and Coote. Fracture in the pipe tests occurred by ductile tearing; a mode of failure the COD Design Curve is not meant to treat. Fracture by tearing is governed by the driving force and resistance to ductile crack growth. Irwin's model for the CTOD of a deep surface crack (c.f. [B6]) can be used to show that the increase of CTOD with crack length is given by

$$\frac{d\delta}{da} = \frac{2\sigma_o}{E}\frac{\ell}{t} .$$

Table B.2 Elastic-Plastic Crack Geometry Correction Factors for Short Surface Defects in Comparison to Elastic Correction Factors; a/t=0.25 in all cases

Internal Pressure (lb/in^2)	Average Stress (ksi)	Strain (%)	a/2c	$\delta_{CCP}(10^{-3}in)$	$\delta(FEM)(10^{-3}in)$	δ_{PT}/δ_{CCP}	Elastic-Plastic $\bar{a}/t$	Elastic $\bar{a}/t$
2500	27.5	0.092	0.167	1.72	1.76	1.02	0.25	0.27
4500	49.5	0.218	0.167	7.93	6.72	0.85	0.21	0.27
2500	27.5	0.092	0.250	1.72	1.46	0.85	0.21	0.22
4500	49.5	0.218	0.250	7.93	5.28	0.67	0.17	0.22
2500	27.5	0.092	0.333	1.72	1.19	0.69	0.17	0.18
4500	49.5	0.218	0.333	7.93	4.28	0.54	0.14	0.18

Thus, the driving force for tearing increases with surface crack length. It is also possible that differences in constraint associated with short and long defects will affect the material resistance to tearing, although the way in which it is affected is not clear.

Finally, we note that because the failure strains for the pipes were in excess of 80% of the uniaxial yield strain some of the data used to generate the modified correction curves are probably better characterized by plastic collapse criteria.

Conclusions

Glover and Coote [B2] have observed a nonuniform factor of safety on strain with surface defect aspect ratio when the COD Design Curve is applied to pipe bending fracture data using linear elastic correction factors for defect geometry. The factor of safety is relatively small for long flaws and relatively large for short flaws. This nonuniformity can be explained by plasticity effects on the defect geometry correction factors. The elastic-plastic estimation approach was used to show that for long flaws, modeled by the SEN geometry, the elastic-plastic correction factors can be substantially greater than those given by elastic analysis. Consideration of solutions for internal, circumferentially cracked cylinders in tension indicates that the actual corrections are not as great as predicted by consideration of the SEN geometry, but that they are still greater than the elastic corrections. A set of numerical data for CTOD of surface defects in pressure vessels was used to assess the elastic-plastic correction factors for short defects. These results suggest that the elastic-plastic correction factors are smaller than the elastic correction factors.

Though plasticity accounts for the trend of the nonuniform safety factor, there may be other explanations. In particular, since the pipes failed by ductile tearing, there is a higher driving force for tearing for long defects. Plastic collapse as a mode of fracture may also influence the computed factors of safety.

REFERENCES

B1. Kamath, M.S., "The COD Design Curve: An Assessment of Validity Using Wide Plate Tests," Int. J. Pres. Ves. and Piping, 9(1981)79-105.

B2. Glover, A.G. and Coote, R.I., "Full-Scale Fracture Tests of Pipeline Girth Welds," in Circumferential Cracks in Pressure Vessels and Piping - Vol. II., PVP - Vol. 95, G. Wilkowski, Ed. (New York; Amer. Soc. Mech. Engr.) 1984, pg. 107-121.

B3. Kumar, V., German, M.D. and Shih, C.F., "An Engineering Approach for Elastic-Plastic Fracture Analysis," Rep. NP-1931, Electric Power Research Inst., Palo Alto, CA (1981).

B4. Newman, J.C., Jr. and Raju, I.S., "Analyses of Surface Cracks in Finite Plates Under Tension and Bending Loads," NASA Tech. Paper 1578(1979).

B5. Erdogan, F., "Theoretical and Experimental Study of Fracture in Pipelines Containing Circumferential Flaws," Report DOT-RC-82007, Lehigh U. (Aug. 1982).

B6. Paris, P.C., "A Method of Application of Elastic-Plastic Fracture Mechanics to Nuclear Vessel Analysis," Appendix B, NUREG-0744, Vol 1, Rev. 1 (Oct. 1981) B1-B48.

B7. Wilkening, W.W., deLorenzi, H.G. and Barishpolsky, M., "Elastic-Plastic Analyses of Surface Flaws in a Reactor Vessel," Trans. ASME, J. Pressure Vessel Technology, 106 (Aug. 1984) 247-254.